Proceedings of the 21st ICSMGE, Vienna, Austria, 14 – 19 June 2026. Pistrol, Adam & Schweiger (eds.)
Published by: ÖGG, Austrian Society for Geomechanics, Salzburg, Austria, ISBN 978-3-9503898-4-5
https://doi.org/10.53243/ICSMGE2026-889

Effect of sample preparation on shear and compression behaviour of clays

Abdullah Ekinci
Associate Professor, Civil Engineering Program, Middle East Technical University, Northern Cyprus Campus, Kalkanli, Guzelyurt, Turkey. ekincia@metu.edu.tr

Hamza Saeed
Post-Doctoral Researcher, Civil Engineering Program, Middle East Technical University, Northern Cyprus Campus, Kalkanli, Guzelyurt, Turkey. saeed@metu.edu.tr

ABSTRACT: Beneficial reuse of unsuitable fine-grained soils in earthworks is often constrained by uncertainty in laboratory-derived strength and compressibility parameters, particularly when in-situ clays occur as aggregated peds rather than fully remoulded material. This study investigates the strength and compression characteristics of specimens prepared using various sample preparation techniques to determine which method best replicates in-situ behaviour. In-situ materials were tested under one-dimensional compression and unconfined compressive strength (UCS) test conditions to evaluate the structural effects of different clay ped sizes. The soil was either finely ground or chopped into discrete peds, with both types subsequently compacted using static uniaxial compaction. X-ray imaging was utilised to examine the pore structure of the compacted specimens. The results indicate that the compression curves for ped-compacted specimens are positioned to the right of those for ground specimens and progressively approach the intrinsic compression line as the ped size increases. Ped-compacted samples demonstrated greater stiffness up to the yield point, after which their behaviour converged toward the intrinsic compression line. UCS tests revealed an inverted-U-shaped trend corresponding to the different ped sizes, where the smaller and intermediate clay peds exhibited higher UCS. As the clay ped sizes increased, a decline in strength occurred, which was also evident through X-ray radiographs exhibiting a higher pore structure.

KEYWORDS: Clay peds, Soil structure, One-dimensional compression, X-ray imaging.

1 INTRODUCTION

The critical state framework is a fundamental concept in soil mechanics that explains soil behaviour under sustained loading involving both compression and shear. In its classical form, the framework suggests that, with sufficiently large plastic strains, soils tend toward unique limiting relationships, commonly represented by a Critical State Line (CSL) and a Normal Compression Line (NCL) (Coop, 2015). Although this principle is well established for reconstituted clays, its applicability becomes less certain for natural or structured soils, in which convergence toward intrinsic reference lines may be delayed, incomplete, or not achieved within typical laboratory stress and strain ranges (Ferreira and Bica, 2006; Todisco and Coop, 2019).

Soils that exhibit incomplete or non-convergent behaviour are often described as transitional soils. Experimental evidence indicates that their tendency to converge toward intrinsic CSLs or NCLs is strongly controlled by initial fabric, bonding, and density, leading to behaviour that departs from the assumptions of classical critical state theory (Xu and Coop, 2016). This divergence is not simply a consequence of inadequate testing. Rather, it reflects persistent internal bonding and particle arrangements that resist homogenisation even after substantial straining (Coop, 2015). As a result, establishing unique intrinsic reference lines for natural soils can be difficult, and the inferred parameters may depend on the preparation and loading path (Ferreira and Bica, 2006). The progression toward convergence is also strain-dependent. Plastic volumetric strain has been shown to be more effective than shear strain in driving destructuring, which is the gradual breakdown of internal fabric toward an intrinsic state (Todisco and Coop, 2019). However, destructuring is frequently incomplete within the limits of standard laboratory testing, particularly for structured clays that retain their internal arrangement even under high loads (Mohamadi et al., 2017).

A key factor governing these responses is the size and integrity of clay peds. Larger peds tend to preserve the original microstructure and promote heterogeneity, thereby slowing destructuring and delaying convergence toward intrinsic behaviour. In contrast, reducing ped size through remoulding or mechanical breakdown promotes homogenisation and can accelerate convergence (Oualmakran and François, 2016; Xu and Coop, 2016). For example, Ekinci (2016) reported that minimising ped size in compacted Lambeth Group clay improved repeatability and reduced structural effects across tests. More generally, the specimen preparation method has a major influence on the behaviour observed during testing. Slurry deposition disperses particles and removes inherited fabric, often producing uniform and reproducible intrinsic responses in critical state testing (Coop, 2015). Conversely, preparation methods such as compaction or moist tamping, although more representative of field placement conditions, may retain bonding, aggregated structures, and macro-voids that impede convergence (Ferreira and Bica, 2006; Liu et al., 2013).

To address these complexities, constitutive models have been developed to represent structure and destructuring. The Structured Cam Clay (SCC) model and related formulations introduce internal variables that evolve with plastic strain to capture gradual structure degradation (Carter and Liu, 2005; Suebsuk et al., 2011). Further developments incorporate structure-dependent friction angles, evolving stress-dilatancy relationships, and anisotropic parameters supported by experimental and numerical observations (Liu et al., 2013; Mohamadi et al., 2017; Mendoza and Farias, 2020).

Previous studies, therefore, highlight that soil structure and specimen preparation can strongly influence convergence and destructuring. In this context, the present research examines how the reconstitution method and the resulting fabric in compacted clay specimens affect convergence behaviour and the transition toward a Intrinsic Compression Line (ICL), with particular emphasis on the role of ped size. The objectives are to establish a reliable convergence criterion and to develop relationships that quantify the links between convergence, destructuring, and the fabric formed during reconstitution. By identifying a specimen preparation protocol that best preserves ped-scale fabric, this study aims to provide more representative strength and compressibility parameters to support the safe, beneficial reuse of unsuitable soils in engineered applications.

2 MATERIALS AND METHODOLOGY

Disturbed alluvial clay was collected from the Long Beach area in the İskele District of Cyprus for laboratory testing, and the index properties are summarised in Table 1. The bulk material was gently disaggregated to form aggregates, referred to as clay "peds", in order to retain ped-scale fabric. The peds were classified into three nominal size classes, small (approximately 3.35 mm), medium (5 to 10 mm), and large (18 to 20 mm). Specimens were prepared under controlled conditions to achieve target initial void ratios (e_o) ranging from 0.527 to 0.722, selected to evaluate the influence of initial density on convergence behaviour.

One-dimensional compression tests were conducted using standard oedometer cells with ring diameters of 30 mm, 50 mm, and 76 mm. Ring sizes were matched to the ped class to represent packing and deformation more reliably while minimising boundary and scale effects. Unconfined compressive strength (UCS) specimens were 50 mm in diameter and 100 mm in height. UCS specimens were prepared by static uniaxial compaction to a constant target dry density of 1.6 g/cm^3 at a moulding water content of 24.17%, which corresponds to the wet side of the compaction curve. Two compaction stress levels were applied, 200 kPa and 400 kPa, using the same procedure for all specimen groups.

Table 1. Index properties of alluvial clay (Ekinci et al., 2022)

Properties	Values
Liquid Limit, *LL* (%)	46
Plastic Limit, *PL* (%)	20
Plasticity Index, *PI* (%)	26
Specific Gravity, G_s	2.66
Sand content (0.075 mm < *D* < 4.75 mm)	6
Silt content (0.002 mm < *D* < 0.075 mm)	54
Clay content (*D* < 0.002 mm)	40
USCS classification	CL
Optimum water content, *w.c.* (%)	17
Maximum dry density, $\rho_{d,\,max}$ (g/cm^3)	1.8

3 RESULTS AND DISCUSSION

Figure 1(a-d) illustrates the one-dimensional compression response as a function of ped size, compaction history, and initial void ratio. Small-ped (SP) specimens (Figure 1-a) show closely clustered e-log(σ'_v) curves across different ring diameters and progressively converge toward lower void ratios with increasing effective vertical stress. Mechanistically, reducing bulk clay lumps to small aggregates decreases meso-scale voids and improves packing uniformity, so early compression is dominated by closure of small inter-ped pores and particle rearrangement, rather than collapse of large fabric features. The resulting reduction in heterogeneity limits stress arching and diminishes persistent inter-ped slip planes, thereby promoting faster destructuring and a more rapid approach toward the intrinsic compression response.

Medium-ped (MP) specimens display greater variability in e-logσ'_v curves (Figure 1-b). This response reflects the coexistence of inter-ped macro-voids and compaction-induced anisotropy. Initial compression is governed by progressive collapse of larger inter-aggregate pores, frictional sliding along ped interfaces, and partial breakage of weak physico-chemical bonds. A more pronounced structural yield stress (σ'_Y), is therefore inferred. With continued loading, bond breakage and fabric realignment intensify and convergence improves, although persistent spacing between curves indicates that part of the meso-structure remains, keeping the compression paths above the intrinsic line within the tested stress range.

Large-ped (LP) specimens (Figure 1-c) start from higher e_o and follow distinct, nearly parallel compression paths over the full stress range. This near-parallelism indicates a relatively constant virgin compression index (C_C), and limited progression toward intrinsic behaviour, which is consistent with transitional fabric. In this case, large inter-ped voids and strong heterogeneity in stress transfer promote arching and kinematic constraints. Deformation localises at ped contacts and along interfaces, so macro-structure collapse remains incomplete even at elevated σ'_v. As a result, the structured compression response remains separated from the intrinsic reference.

The fully reconstituted material provides the intrinsic reference state, represented by a single smooth e-log(σ'_v) curve that defines the intrinsic compression line (ICL) and is free of structural memory. The combined plot (Figure 1-d) summarises the overall progression. SP specimens approach a relatively unique compression path as meso-scale features are minimised. MP specimens show partial to near-complete convergence as macro-voids and interface effects are progressively removed. LP specimens retain a strong structural influence, and macro-voids and interfaces delay or prevent convergence within the applied stress range. Overall, ped size governs the balance between macro-void collapse, inter-ped contact mechanics, and bond breakage during compression. Smaller peds promote homogeneous packing, reduce the apparent structural yield stress, and accelerate destructuring toward the ICL. Larger peds preserve fabric-scale heterogeneity, sustain arching and interface sliding, and maintain a distinct structured response even under higher effective vertical stresses.

To quantify convergence across ped classes, an *m*-slope analysis was performed by regressing the void ratio at selected effective vertical stresses against the initial void ratio. This relationship is expressed as $e = m\, e_o + c$ (Table 2). Values of *m* approaching zero indicate convergence toward a unique normal compression response, whereas $m > 1$ indicates divergence, meaning that differences in e_o are amplified with loading.

For SP specimens, *m* decreases from 0.82 at 55 kPa to 0.47 at 1760 kPa, indicating steady convergence with increasing stress, while maintaining some dependence on e_o. For MP specimens, *m* decreases more sharply, from 0.88 to -0.08, indicating strong destructuring and near-complete convergence at high stress. The negative slope reflects crossover behaviour, in which initially looser specimens compress more, reversing the influence of initial density. In contrast, LP specimens retain $m > 1$ across the stress range, indicating divergence and persistence of the initial fabric.

To characterise progressive fabric breakdown using a single normalised metric, a stress-dependent destructuring function was defined from the evolution of the *m*-slope (Equation 1), using the lowest stress level in the programme as the reference state (55 kPa in this study). When plotted against σ'_v (Figure 2), the resulting index enables direct comparison of destructuring rates across ped categories. Steeper D-log(σ'_v) trajectories indicate rapid structural breakdown at relatively low stresses, whereas flatter trajectories indicate slower breakdown and stronger transitional behaviour. Operationally, the function enables threshold-based interpretation. For example, if a target destructuring level is set, the corresponding stress required to reach that level can be read directly from the curve, providing a basis for setting preloading or compaction targets. The inflection point of the D-log(σ'_v) curve further indicates the transition from fabric-controlled response toward near-intrinsic behaviour.

$$D\,(\sigma'_v) = 1 - \frac{m_{(\sigma'_{v,i})}}{m_{(\sigma'_{v,low-stress\ level})}} \tag{1}$$

where $m_{(\sigma'_{v,i})}$ is the m-slope at a given stress level and $m_{(\sigma'_{v,low-stress\ level})}$ is the reference *m*-slope value at the lowest

applied stress (e.g. 55 kPa in this study). The Equation 1 formulation yields a dimensionless destructuring index, $D(\sigma'_v)$, $\in [0, 1]$. By definition, $D(\sigma'_v) = 0$ denotes no destructuring, with structural influences fully retained, and $D(\sigma'_v) = 1$ denotes complete destructuring of initial fabric, consistent with convergence toward a unique compression line.

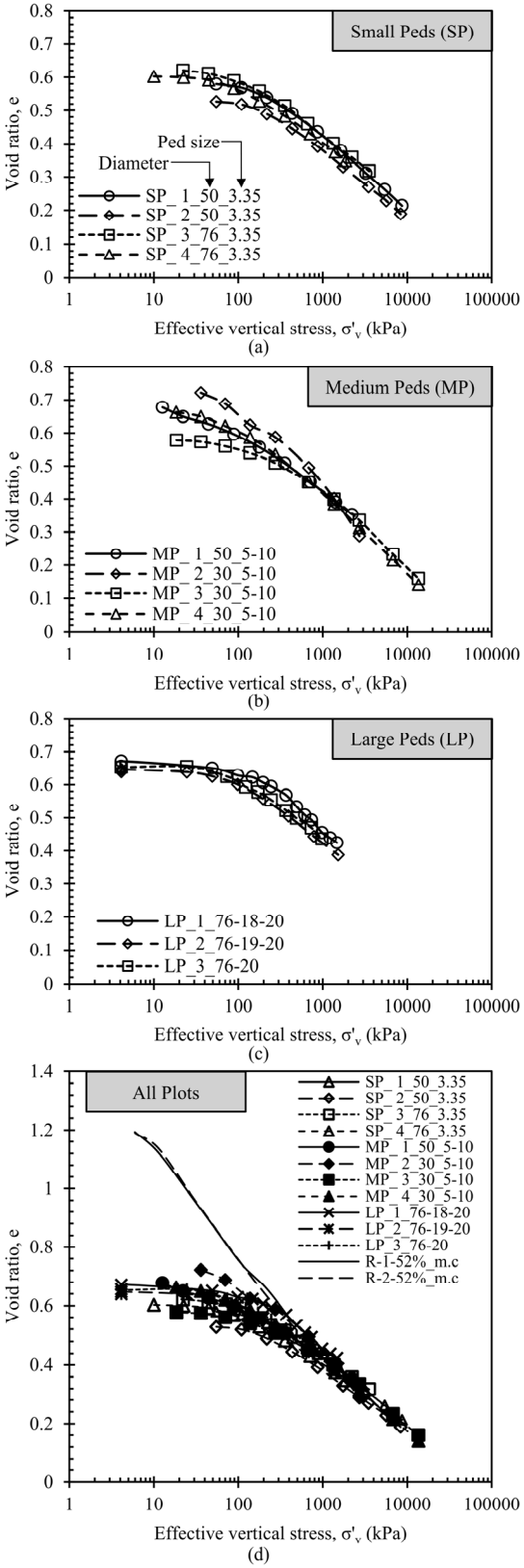

Figure 1. One-dimensional compression curves of (a) SP, (b) MP, (c) LP, and (d) all plots with reconstituted specimens.

Table 2. m-slope convergence criteria of (a) SP, (b) MP, and (c) LP.

Stress Level (kPa)	Small Peds	Medium Peds	Large Peds
0	y = x	y = x	y = x
55	y = 0.8163x+0.0991	y = 0.8832x+0.0475	y = 1.3215x+0.2227
110	y = 0.6175x+0.1968	y = 0.6594x+0.1610	y = 1.3947x-0.2979
220	y = 0.5404x+0.2082	y = 0.5089x+0.2198	y = 2.2438x-0.8858
440	y = 0.4980x+0.1862	y = 0.3859x+0.2529	y = 2.2889x-0.9689
880	y = 0.4601x+0.1529	y = 0.1830x+0.3225	y = 1.6862x-0.6491
1760	y = 0.4678x+0.0870	y = -0.0789x+0.4240	

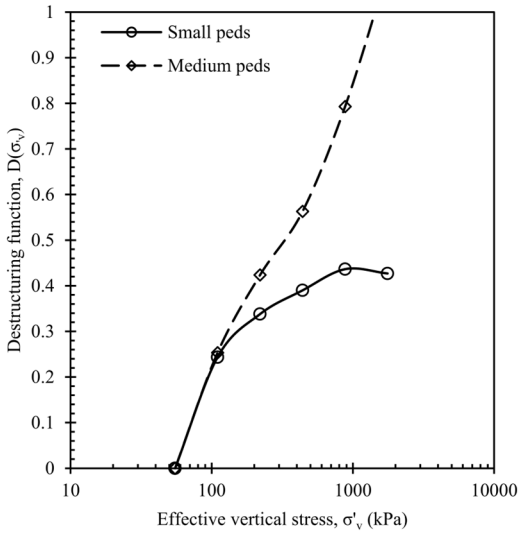

Figure 2. Destructuring curves of different ped classes.

For design applications, the destructuring function can be used to interpolate compressibility parameters, such as C_C or coefficient of volume compressibility (m_v), between structured and intrinsic states using a weighted formulation (Equation 2). This provides a practical route for incorporating progressive destructuring into settlement estimation, particularly for compacted or treated clays in which the in-service stress path drives gradual fabric breakdown.

$$C_{c,actual} = (1 - D)C_{c,structured\ fabric} + D\ C_{c,intrinsic} \qquad (2)$$

UCS results show an inverted U-shaped trend with ped size for both compaction stress histories (200 kPa and 400 kPa), as presented in Figure 3. UCS increases from the smallest ped sizes to approximately 4 mm, then decreases toward the largest ped sizes. In the 400 kPa series, UCS increases from 25.4 kPa at 0.5 mm to a peak of 46.1 kPa at 4 mm (an 82 percent increase), then decreases to 32.9 kPa at 12 mm (a 29 percent reduction from the peak). In the 200 kPa series, UCS increases from 26.0 kPa to 48.8 kPa at 4 mm (an 88 percent increase), then decreases to 23.5 kPa at 12 mm (a 52 percent reduction from the peak). A quadratic model captures this non-monotonic behaviour with R^2 =0.88 for the 400 kPa series and R^2=0.70 for the 200 kPa series. The inferred optimal ped-size window, approximately 5 to 6 mm, likely reflects a balance between dense contact networks and continuity of ped bonding, while limiting macro-voids and weak interface planes. In addition, the optimum ped size was computed as D = -b/(2c) with a corresponding predicted peak strength derived from a quadratic function. Overall, the Figure 3 plot indicates an optimal clay ped size window for UCS and highlights that excessive ped size preserves meso-structure, which undermines peak strength even under higher applied stress.

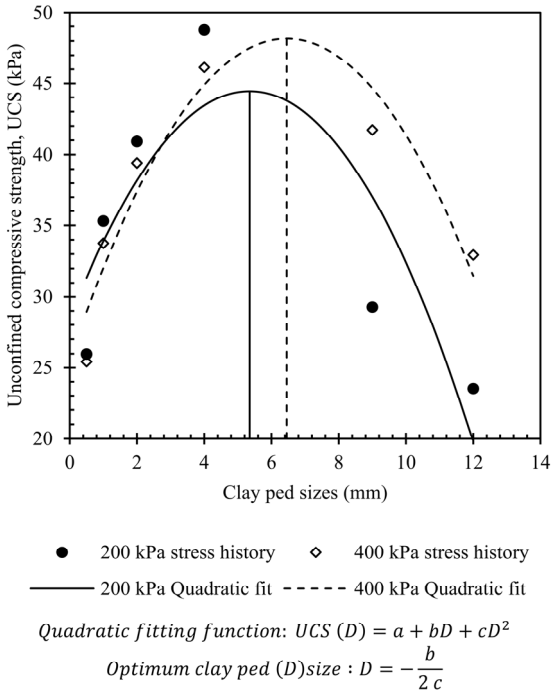

Figure 3. UCS variation with respect to clay ped size and stress history.

X-ray radiographs (Figure 4) provide microstructural evidence supporting the UCS trend. For small peds (approximately 0.5 to 2 mm), the radiographs show pronounced mottling and faint longitudinal banding, indicating locally variable density and clusters of meso-voids that disrupt contact continuity, which is consistent with moderate UCS. At intermediate ped sizes (around 4 mm), the radiographs appear more uniform, suggesting a well-connected contact network with fewer macro-voids and limited interface planes, consistent with peak UCS. At larger ped sizes (approximately 9 to 12 mm), axial streaks and brightness patches become more apparent, indicating the development of ped-to-ped interface planes and macro-voids. These features promote stress arching and facilitate early crack initiation, explaining the post-peak reduction in UCS despite comparable average density. Table 3 summarises key radiographic features and their correspondence with UCS behaviour.

Table 3. Comparative X-ray fabric signatures and UCS outcomes for different ped sizes.

Ped size	X-ray dominant features	Fabric interpretation	UCS behaviour
Small peds	Noticeable mottling, faint banding, higher greyscale dispersion	Micro void clusters; local density variability	Moderate UCS, strength limited by microscale heterogeneity
Medium peds	Smooth greyscale, minimal streaks, uniform appearance	Well-connected contact network, low macro-void network	Peak UCS, optimal balance of contact points and fabric continuity
Large peds	Mottling and longitudinal banding, bright patches	Ped-to-ped interfaces and macro void clusters	UCS post-peak decline

4 CONCLUSION

The study evaluated the convergence and structural breakdown of compacted alluvial clay with varying clay ped sizes by one-dimensional compression and UCS tests. The following are the key conclusions of this study:

- In terms of compression behaviour, small clay peds demonstrated moderate convergence toward their intrinsic compression behaviour. Medium peds showed significant destructuring and apparent convergence at intermediate effective stresses. In contrast, large peds retained elements of their initial fabric and displayed transitional behaviour, even under higher stresses.
- To facilitate consistent comparison across different ped classes, a destructuring function was proposed. This function provides a normalised (0-1) measure of structural breakdown.
- Unconfined compressive strength varies in a non-monotonic manner with clay ped size, displaying an inverted U-shape. When compared to a ped size of 0.5 mm, the strength increases by approximately 82% (to 400 kPa) and about 88% (to 200 kPa) at the peak. However, as the clay ped size increases to 12 mm, the strength decreases by roughly 29% and 52%, respectively. Intermediate ped sizes optimise contact density and continuity, while very small ped maintain micro-scale heterogeneity. Conversely, larger peds create macro-voids and interface planes that localise stress and reduce strength.
- Additionally, higher compaction stresses (400 kPa) result in a more stable response with a gentler decline after reaching the peak strength. In contrast, the 200 kPa series experiences a more significant loss of strength at larger ped sizes.
- In X-ray radiographs of intermediate-sized peds, a smooth grayscale is observed with minimal streaking. This indicates a well-connected contact network that corresponds to the maximum unconfined compressive strength. In contrast, large peds exhibit mottling and longitudinal banding, which suggest the presence of ped-to-ped interfaces and macro-voids; these characteristics account for the decrease in unconfined compressive strength at larger sizes. Small peds display noticeable mottling that reflects local density variations and clusters of micro-voids, which align with a moderate unconfined compressive strength rather than the peak strength.
- The results demonstrate that compression and unconfined compressive strength are governed by the extent of in-situ ped-scale structure preserved during sampling and specimen preparation; greater remoulding progressively shifts the response toward an intrinsic (fully destructured) state.
- A stress-dependent destructuring function was established to quantify structure loss with loading, and this was then used within a compression-index relationship to express the measured compression index as a transition between a structured-fabric end-member and an intrinsic end-member, providing a practical basis for selecting preparation protocols when laboratory parameters are intended to represent field behaviour.

(a)

(b)

Figure 4. X-ray radiographs of specimens with varying ped sizes.

5 REFERENCES

Coop, M., 2015. Limitations of a critical state framework applied to the behaviour of natural and "transitional" soils. In: Deformation characteristics of Geomaterials. IOS Press, pp.115–155.

Ekinci, A., Ferreira, P.M.V. and Rezaeian, M., 2022. The mechanical behaviour of compacted Lambeth-group clays with and without fibre reinforcement. Geotextiles and Geomembranes, 50(1), pp.1–19.

Ferreira, P.M.V. and Bica, A.V.D., 2006. Problems in identifying the effects of structure and critical state in a soil with a transitional behaviour. Géotechnique, 56(7), pp.445–454.

Liu, W., Shi, M., Miao, L., Xu, L. and Zhang, D., 2013. Constitutive modeling of the destructuration and anisotropy of natural soft clay. Computers and Geotechnics, 51, pp.24–41.

Mendoza, C. and de Farias, M.M., 2020. Critical state model for structured soil. Journal of Rock Mechanics and Geotechnical Engineering, 12(3), pp.630–641.

Mohamadi, M., Wan, R. and Shen, Z., 2018. An elastoplastic description of frictional destructuration in natural clays and shales. Acta Geotechnica, 13(4), pp.911–924.

Oualmakran, M., 2016. Multi-scale behaviour of aggregated soils: Experimental characterisation and Constitutive modelling. Unpublished doctoral dissertation. Université libre de Bruxelles, Ecole polytechnique de Bruxelles – Constructions, Bruxelles.

Suebsuk, J., Horpibulsuk, S. and Liu, M.D., 2011. A critical state model for overconsolidated structured clays. Computers and Geotechnics, 38(5), pp.648–658.

Todisco, M.C. and Coop, M.R., 2019. Quantifying "transitional" soil behaviour. Soils and Foundations, 59(6), pp.2070–2082.

Xu, L. and Coop, M.R., 2016. Influence of structure on the behavior of a saturated clayey loess. Canadian Geotechnical Journal, 53(6), pp.1026–1037.